Vibrational Monitoring of Isolated Targets Using Single-Pass SAR Images

CHIARA SUPPI, ALESSANDRO LOTTI,
ALEKSANTERI VATTULAINEN, SEBASTIAN DIAZ RIOFRIO,
FINLAY ROLLO, CHRISTOS ILIOUDIS, DANIEL TONELLI,
ENRICO TUBALDI, CARMINE CLEMENTE, DANIELE ZONTA
and PIETRO MILILLO

ABSTRACT

This paper presents a method for extracting dynamic information from isolated vibrating targets using a single high-resolution X-band SAR image. The algorithm is based on the micro-motion principle to detect the movement of reflective targets. The method was validated through experimental tests conducted in Trento (Italy) and Glasgow (UK). The results obtained confirm the effectiveness of the algorithm in extracting velocities as low as 0.01 m/s.

INTRODUCTION

Structural Health Monitoring (SHM) plays a crucial role in assessing the condition of structures, enabling the timely identification of potential damage, and the planning of targeted interventions to ensure structural safety. Traditional SHM systems rely on contact-based sensors directly on structures to monitor their responses over time. However, the implementation of these systems presents significant challenges, particularly when deployed on large-scale infrastructure, as they may entail high costs associated with complex configurations and the need for continuous maintenance [1].

In order to overcome these limitations of traditional methods, remote sensing technologies, particularly those based on satellite systems, offer an innovative and non-invasive solution. Since the 1990s, the development of satellites equipped with Synthetic Aperture Radar (SAR) has enabled advanced studies on structural monitoring, thanks to the ability of these instruments to provide high resolution images. Among the most advanced satellite remote sensing techniques, SAR interferometry (InSAR) stands out for its capability to measure displacements along the satellite's Line of Sight (LoS) with millimetric precision [2] [3].

Chiara Suppi, University of Trento, via Mesiano 77, Trento, Italy

Nevertheless, the effectiveness of this technique is constrained by the availability of extensive radar image datasets acquired over the same area, under consistent acquisition modes, and at close temporal intervals which are dictated by satellite revisit times, typically 15-20 days [4]. Furthermore, InSAR techniques do not enable the extraction of dynamic information related to observed targets.

For the above reasons, it is preferable to develop monitoring techniques based on single-pass SAR, capable of extracting dynamic information from vibrating targets. Recent studies have highlighted the efficacy of micro-motion (m-m) analysis for evaluating such information. In [5], a m-m technique is proposed for the structural monitoring of a dam, while in [6], the study of micro-motions has shown the potential for monitoring long-span bridges, albeit without a direct comparison to ground-acquired data. Finally, [7] discuss feasibility and limitations of m-m sensing from SAR sensors.

This paper proposes an algorithm, similar to [6], designed to extract vibrational information from a single SAR image by leveraging micro-Doppler (m-D) frequency shifts in the received SAR signal caused by the m-m of vibrating targets. Micro-Doppler generates artifacts in the final radar image, known as paired echoes, where the ground target appears blurred and shifted in multiple positions along the azimuth direction, resulting in a "ghost target" effect [8].

The proposed algorithm was validated using high resolution X-band SAR data acquired by the Umbra satellite constellation [9]. The extracted results were compared against ground-truth measurements collected during in situ tests synchronized with satellite overpasses. Experimental campaigns were conducted in Trento (Italy) and Glasgow (UK), employing a controlled single-degree-of-freedom oscillator subjected to various excitation signals, including sinusoidal inputs, signal superpositions, and linear frequency sweeps.

The structure of the paper is as follows: Section 2 introduces the principles underlying the developed algorithm and describes its pipeline, Section 3 presents the case study, Section 4 analyzes the results, and Section 5 summarizes the conclusions of the study.

METHOD

The proposed algorithm processes Single Look Complex (SLC) images formatted according to Sensor Independent Complex Data (SICD) format, which includes the SLC image along with associated metadata describing imaging geometry and radar parameters [10].

The used radar image is referenced in the slant plane which is a two-dimensional reference frame defined by the range (or radial) direction, aligned along the satellite's Line of Sight (LoS), and the azimuth direction, corresponding to the flight path of the satellite. The image is a matrix of complex-valued pixels, encoding both amplitude and phase information of the backscattered radar signal. Data acquisition was performed in spotlight mode, whereby the radar sensor continuously illuminates the scene over a specified time interval, allowing the target to be observed from multiple viewing angles. This enables high resolution in azimuth directions. Notably, the azimuth resolution, critical for micro-motion extraction, is directly proportional to

the synthetic aperture duration: the longer the observation time, the finer the achievable resolution.

Standard SAR processing methods assume that the observed scene is static. However, moving targets induce phase modulation in the backscattered radar signal, which can result in image artefacts such as smearing, paired echoes, and misregistration in the final image. In particular, a target moving with constant radial velocity relative to the platform will appear displaced along the azimuth direction, and its offset in the SAR image can be estimated as follows [11]:

$$\Delta x = \frac{v_r \cdot R}{V} \tag{1}$$

where Δx is the azimuth distance in meters, v_r is the radial velocity of the target, V is the velocity of the platform, and R is the slant range distance to the target point.

In the case of vibrating targets, the continuous change in velocity direction produces symmetric echoes along the azimuth axis, commonly known as 'ghost targets' [8].

The proposed algorithm estimates the time series of the radial velocity of vibrating targets by analyzing the azimuthal displacement of ghost targets induced by the m-D effect. To reconstruct the motion dynamics, the SAR image is segmented into sub-aperture (SA) images, each corresponding to a distinct time interval within the total observation period (t_{obs}).

The sub-aperture process critically depends on the appropriate selection of the following parameters:

- **Aperture Fraction** (AP): Defines the percentage of the full-aperture image frequency spectrum used for the reconstruction of each sub-image. A low AP value reduces spectral content, leading to a significant degradation in the spatial resolution of each SA.
- **Overlap** (OL): Specifies the percentage of overlap between consecutive SA images. A high OL value yields highly similar sub-apertures, reducing the algorithm's sensitivity to the target's motion dynamics.
- **Number of Sub-Apertures** (NSA): Represents the total number of SA images extracted from the full-aperture image. It can be computed as a function of AP and OL according to the following relation:

$$NSA = \frac{1 - AP \cdot OL}{AP \cdot (1 - OL)} \tag{2}$$

The number of sub-apertures must be greater than or equal to the minimum number of samples dictated by the Nyquist sampling theorem, applied to the bandwidth B of generated signal:

$$NSA_{min} = 2 \cdot B \cdot t_{obs} < NSA \tag{3}$$

Careful optimization of AP, OL, and NSA is essential to achieve an effective trade-off between spatial resolution, given by $d_s = AzSS/AP$, where $AzSS$ is the full-aperture azimuth resolution, and temporal resolution, defined as $d_t = t_{obs}/NSA$. The trade-off is key to ensuring the quality and reliability of vibrational analysis.

According to the above considerations, the overall processing pipeline for radial velocity extraction is structured as follows:

1. **Region of Interest selection** (RoI): The spatial-domain image is cropped around the target area, ensuring that the target motion is fully captured. This step helps reduce computational costs.
2. **2D Fourier Transform** (2D-FFT): The RoI is transformed into the frequency domain using a two-dimensional Fast Fourier Transform. This results in the spectral matrix of the full-aperture image.
3. **Sub-Aperture generation**: The spectral matrix is divided into multiple sub-apertures along the azimuth direction, maintaining a fixed AP and OL. This process produces N sub-apertures according to Equation (2).
4. **2D Inverse FFT** (2D-IFFT): Each of the N sub-apertures is processed using a two-dimensional Inverse Fast Fourier Transform to reconstruct a series of range-azimuth images at reduced resolution.
5. **Pixel tracking**: The azimuthal displacement of the brightest pixel in each sub-aperture is identified and tracked over time.
6. **Radial velocity estimation**: The azimuthal pixel displacement is converted into radial velocity using Equation (1) along with SAR metadata (satellite velocity, slant range distance, azimuth resolution).
7. **Spectral analysis**: The resulting radial velocity signal is analyzed via FFT to extract dominant vibration frequencies.
8. **Performance evaluation**: Three quantitative metrics are used to evaluate the algorithm's performance by comparing the extracted signal to the in situ reference: the Pearson correlation coefficient, the standard deviation of the difference, and the signal-to-noise ratio.

The proposed pipeline has been tested in controlled and real-world settings, and further details are provided in the next section.

CASE STUDY

The objective of the experimental trials was to assess the algorithm's capability to detect and reconstruct vibrational signatures from an isolated target. The algorithm was validated through an experimental campaign conducted at Villa Gherta in Trento (Italy) and at Glasgow Green in Glasgow (United Kingdom). These locations were specifically selected for their open and low-clutter environments, in order to minimize interference from surrounding structures or reflective objects (Figure 1). The ground target used for testing was created by mounting a Corner Reflector (CR) on an electromechanical shaker (Figure 1). The CR enhanced radar backscatter, improving the signal-to-noise ratio relative to the surrounding environment. During each satellite pass, the shaker reproduced predefined vibration signals, while a Linear Variable Differential Transformer (LVDT) measured the actual ground displacement

of the reflector in real-time. This dual-measurement strategy enabled cross-validation between ground truth and SAR-derived outputs.

The vibrational signals used in the experiments covered a range of amplitudes and frequencies to test the robustness of the method under varying dynamic conditions. Table I reports four tests, each referring to a sinusoidal signal generated with a distinct and constant combination of amplitude (A) and frequency (f), selected to produce progressively lower velocities. The maximum vertical vibration velocity of the target, computed as the time derivative of the displacement, is reported in the table under the label Vel.max. Additionally, the table reports relevant metadata associated with the satellite pass for each test. Specifically, it includes the incidence angle (Inc. ang.), required to project the target's vertical velocity onto the satellite's LoS, the azimuth resolution (Az. res.), the slant range distance (Slt. range), and the satellite platform velocity (Plat. vel.); the latter parameters are essential for estimating the Δx position as described in Equation (1).

a) b) c)

Figure 1. a) Location of the test campaign conducted in Italy at Villa Gherta; b) Location of the test campaign conducted in Glasgow at Glasgow Green; c) Corner reflector and LVDT

TABLE I. Ground signal properties and satellite metadata

Test ID	Type	A (m)	f (Hz)	Vel. max (m/s)	Inc. ang. (°)	Az. res. (m)	Slt. range (m)	Plat. vel. (m/s)
1	Sin.	0.045	1.00	0.282	43.39	0.22	709490.87	7672.50
2	Sin.	0.024	1.00	0.152	54.80	0.22	843760.13	7685.85
3	Sin.	0.005	2.00	0.066	54.84	0.22	865808.35	7670.42
4	Sin.	0.003	2.00	0.040	49.36	0.22	715797.72	7695.79

RESULTS

The velocity time series extracted using the proposed algorithm are presented and compared with those acquired on-site. The comparison is carried out in both the time and frequency domains. Table II reports the input parameters used by the algorithm to reconstruct the time series from the satellite acquisitions. The same table also summarizes the main comparison results, expressed in terms of correlation coefficient (ρ), standard deviation of the difference (σ), and signal-to-noise ratio (SNR).

Letting x denote the reference signal acquired from the ground sensor and y the signal extracted through the algorithm, the correlation is evaluated using Pearson's coefficient, defined as:

$$\rho(x,y) = \frac{1}{N-1}\sum_{i=1}^{N}\left(\frac{x_i-\mu_x}{\sigma_x}\right)\left(\frac{y_i-\mu_y}{\sigma_y}\right) \tag{4}$$

where μ_x and μ_y are the mean values, σ_x and σ_y the standard deviations of the two signals, and N the number of samples.

To quantify the dispersion between the signals, the standard deviation of the pointwise difference is computed as:

$$\sigma(x,y) = \sqrt{\frac{1}{N-1}\sum_{i=1}^{N}[(x_i-y_i)-\mu_\Delta]^2} \tag{5}$$

where μ_Δ is the mean of the differences $(x_i - y_i)$.

Finally, the signal-to-noise ratio is estimated according to the expression:

$$SNR = 10\,log_{10}\left(\frac{\sum_{i=1}^{N}x_i^2}{\sum_{i=1}^{N}(x_i-y_i)^2}\right) \tag{6}$$

TABLE II. m-m extraction parameters and results

Test ID	t obs. (s)	AP (%)	OL (%)	NSA (-)	ρ (-)	σ (m/s)	SNR (dB)
1	5.21	1.80	0	54	0.98	0.031	13.80
2	6.04	3.60	30.16	39	0.98	0.015	12.86
3	6.11	3.40	64.21	80	0.95	0.009	9.99
4	5.41	4.90	65.05	52	0.70	0.015	2.95

Figure 2 illustrates the results of the comparison between the signals. The orange trace corresponds to the ground signal acquired in situ, whereas the blue trace corresponds to the signal extracted using the algorithm. For each test, the figure shows the velocity time series along the LoS, the corresponding frequency spectrum, and the key performance metrics. To ensure accurate metric computation and comparability between the signals, the blue trace was reconstructed by linearly interpolating the samples obtained from each sub-aperture, resulting in a dataset with the same number of samples as the ground-based signal.

It can be observed that in all the cases presented, the frequency is estimated accurately. However, it is also evident that as the velocity decreases, the accuracy of the amplitude estimation tends to decline.

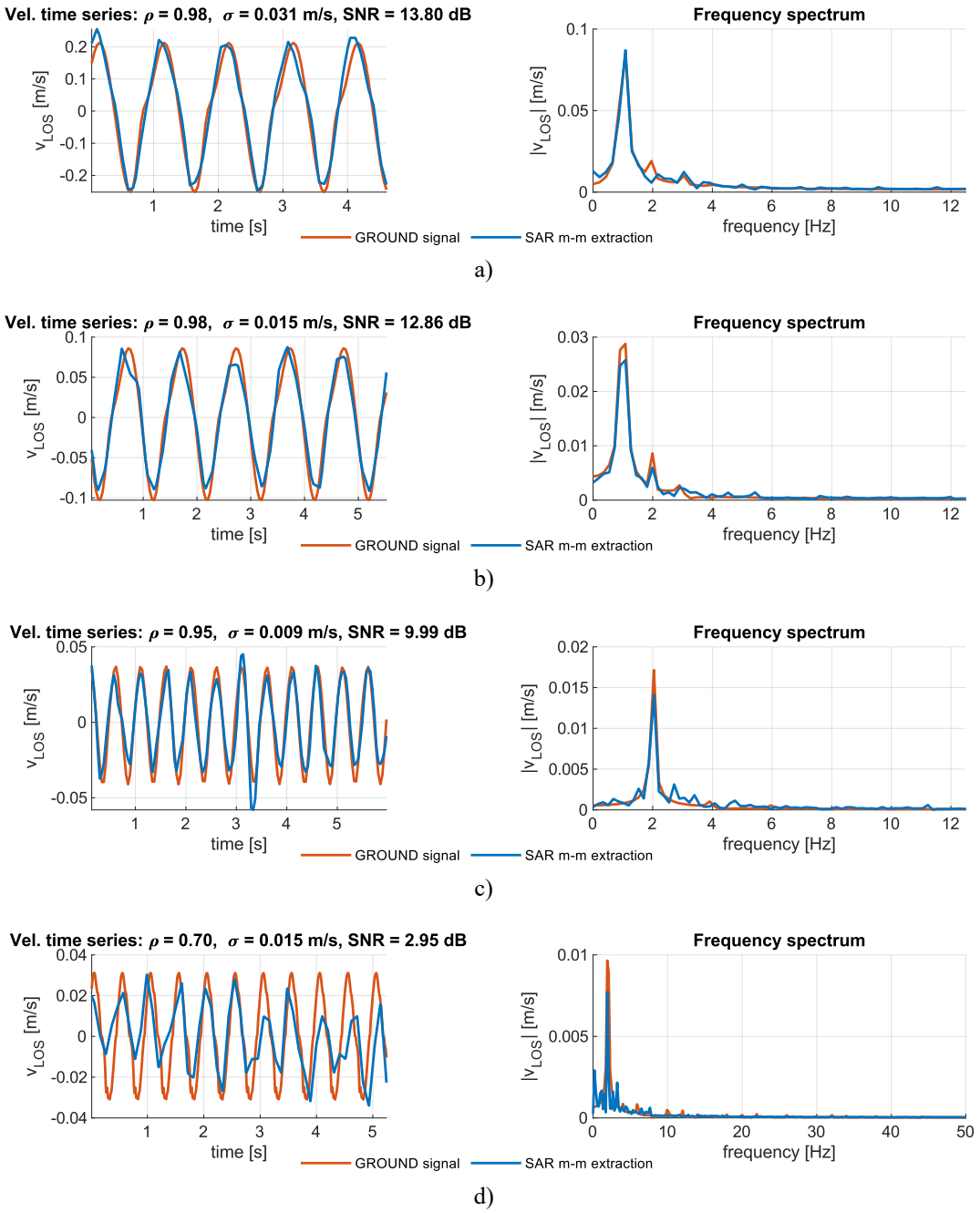

Figure 2. Time series and frequency spectrum of the velocity along the LoS, for: a) Test ID 1, b) Test ID 2, c) Test ID 3, and d) Test ID 4.

CONCLUSIONS

This paper proposed a m-m technique for estimating vibration velocity of targets using single-pass SAR images. The methodology was validated on an ideal case study, involving a single-degree-of-freedom oscillator in a disturbance-free environment. The velocity time series extracted using the technique showed good agreement with ground-acquired data, with correlation coefficients above 0.70 and standard deviations of the difference below 0.031. The most significant errors

occurred when the maximum vibration radial velocity was around 0.01 m/s, highlighting the technique's limitations in detecting low velocities. This issue is linked to the limited azimuth resolution of the initial SAR image, which can be improved by increasing the observation time during radar acquisition.

Future studies will focus on a priori selection of the algorithm's input parameters (AP, OL) and on the optimization of the interpolation function, in order to enhance the accuracy of the reconstructed signal amplitude. Moreover, the technique is expected to be extended to more complex real-world case studies.

ACKNOWLEDGEMENTS

This research was supported by multiple funding sources. The authors gratefully acknowledge the European Space Agency (ESA) for funding the projects "Bridge Monitoring Based on Single Pass SAR Images" and "EO4Security-Innovative SAR Processing Methodologies for Security Applications (Topic B2: Micro-Doppler Processing)". Additional support was provided by the ReLUIS Interuniversity Consortium (DPC-ReLUIS 2020–2022 and 2024–2026, WP6: "Monitoring and Satellite Data"). The study also received funding from the European Union-Next Generation EU (Mission 4, Component 2; CUP: E53D23003560006). The authors extend their sincere gratitude to Umbra for providing satellite imagery and to the Glasgow City Council for authorizing the on-site measurement campaign.

REFERENCES

[1] Brownjohn, J. M. W. 2007. "Structural Health Monitoring of Civil Infrastructure," *Philos. Transact. A Math. Phys. Eng. Sci.*, 365(1851):589–622.

[2] Lazecky, M., D. Perissin, M. Bakon, J. M. de Sousa, I. Hlavacova, and N. Real. 2015. "Potential of Multi-Temporal InSAR Techniques for Structural Health Monitoring."

[3] Ullo, S. L., F. Biondi, P. Addabbo, C. Clemente, and D. Orlando. 2019. "Application of DInSAR Technique to High Coherence Sentinel-1 Images for Dam Monitoring and Result Validation Through In Situ Measurements," *IEEE J. Sel. Top. Appl. Earth Obs. Remote Sens.*, 12(3):875–890.

[4] Perissin, D. 2016. "Interferometric SAR Multitemporal Processing: Techniques and Applications," in *Multitemporal Remote Sensing: Methods and Applications*, pp. 145–176.

[5] Biondi, F., P. Addabbo, C. Clemente, S. L. Ullo, and D. Orlando. 2020. "Monitoring of Critical Infrastructures by Micromotion Estimation: The Mosul Dam Destabilization," *IEEE J. Sel. Top. Appl. Earth Obs. Remote Sens.*, 13:6337–6351.

[6] Biondi, F., P. Addabbo, S. L. Ullo, C. Clemente, and D. Orlando. 2020. "Perspectives on the Structural Health Monitoring of Bridges by Synthetic Aperture Radar," *Remote Sens.*, 12(23):3852.

[7] Clemente, C., et al. 2024. "On Micro-Motion Extraction from High Resolution X-band SAR Products," in *IEEE International Geoscience and Remote Sensing Symposium (IGARSS24)*, pp. 1182–1186.

[8] Ruegg, M., E. Meier, and D. Nuesch. 2007. "Vibration and Rotation in Millimeter-Wave SAR," *IEEE Trans. Geosci. Remote Sens.*, 45(2):293–304.

[9] "Umbra SAR Constellation - eoPortal."
[Online]. Available: https://www.eoportal.org/satellite-missions/umbra-sar#spacecraft

[10] Pierce, L. 2022. "A New Metadata Standard for Single-Look Complex SAR Data," in *IEEE Radar Conference (RadarConf22)*, pp. 1–4.

[11] Raney, R. K. 1971. "Synthetic Aperture Imaging Radar and Moving Targets," *IEEE Trans. Aerosp. Electron. Syst.*, AES-7(3):499–505.